

INTERNATIONAL SOCIETY FOR SOIL MECHANICS AND GEOTECHNICAL ENGINEERING



This paper was downloaded from the Online Library of the International Society for Soil Mechanics and Geotechnical Engineering (ISSMGE). The library is available here:

<https://www.issmge.org/publications/online-library>

This is an open-access database that archives thousands of papers published under the Auspices of the ISSMGE and maintained by the Innovation and Development Committee of ISSMGE.

Cyclic Resistance versus Shear Wave Velocity as Affected by Aging of Sandy Deposits

R. S. Amoly¹, H. Bilsel², and K. Ishihara³

ABSTRACT

Some researchers have reservations about employing small-strain shear-wave velocity in the assessment of medium-to-large strain liquefaction. However, some others confirm that the shear wave velocity is more likely to suit for distinguishing the liquefaction and non-liquefaction susceptibility of sand deposits by the V_s -based liquefaction chart, similar to the other types of indices such as SPT and CPT. Such liquefaction charts have commonly been proposed based on the liquefaction resistance of young Holocene deposits, without taking “age” into account. In an attempt to bridge the gap between two approaches, relations between liquefaction resistance and shear wave velocity of sand deposits are proposed under aging effect using a newly introduced index property, “cyclic yield strain”, to differentiate between new and old sand deposits. It may be concluded, therefore, that this parameter can be employed as a yardstick for taking into account the cementation or the effect of age in sandy soils.

Introduction

The assessment of liquefaction susceptibility during earthquake has been a significant topic for geotechnical engineers in seismically active zones of the world. In carrying out this task, the evaluation of cyclic resistance of sand deposits is of crucial importance.

One of the procedures to accomplish this aim would be to secure undisturbed samples of soils from potentially liquefiable in-situ deposits and to test them in the laboratory under cyclic loading condition. The other method would be to assess the cyclic resistance of in-situ soils via some empirical formulae or charts correlating the cyclic strength with the penetration resistance through in-situ tests such as Standard Penetration Test (SPT) and Cone Penetration Test (CPT). Still, the alternative method would be to make use of shear wave velocity which can be measured in-situ at low cost by means of several procedures without necessarily drilling bore holes. The utilization of such method, however, has a drawback due to the liquefaction being related with medium to large shear strain in contrast to the infinitesimal shear strain involved in the propagation of the shear wave. In spite of such potential shortcomings, there has been an appreciable amount of work done towards the use of shear wave velocity, attempting to establish correlation between the cyclic strength and shear wave velocity such as Dobry et al. (1980), Tokimatsu and Uchida (1990) and Andrus and Stokoe (2000). Thus, if there is some physical

¹Ph.D. Candidate, Civil Engineering Department, Eastern Mediterranean University, Famagusta-Mersin10, Turkey, safaeian.amoly@students.emu.edu.tr

²Associate Professor, Civil Engineering Department, Eastern Mediterranean University, Famagusta-Mersin10, Turkey, huriye.bilsel@emu.edu.tr

³Professor, Research and Development Initiative, Chou University, Tokyo, Japan, Kenji-ishihara@e-mail.jp

interpretation provided for the correlation between them, the use of the shear wave velocity will be justified as a meaningful approach to assess the liquefaction resistance of in-situ deposits of sandy soils.

In an attempt to fill the gap in understanding the relationship between the shear wave velocity involving small strain and the cyclic resistance of sandy soils inducing medium to large shear strain, what might be termed “cyclic yield strain”, or “cyclic reference strain” is introduced.

Several factors may be envisaged to exert influence on the stiffness or softness of soils. One of the factors likely to be associated would be the aging of soil deposits. It is with good reasons to infer that in-situ soils having a long history of deposition may show “stiff” behavior, in contrast to the “soft” response of soils with a short history of deposition. Thus, the effect of aging of soil deposits may be reflected somewhat in the cyclic yield strain. In view of the fact that the larger the cyclic yield strain, the softer the response of soils would be and vice versa, it may be concluded that the cyclic yield strain can be utilized as a yardstick parameter for taking into account the aging effect of sandy soils. It is reasonably conceived that the cyclic yield strain will take larger values for soft fresh deposit and smaller values for stiff old aged deposits of sands.

The objective of this paper is to seek for different curves to correlate the cyclic strength and the shear wave velocity in terms of new and old aged deposits on the basis of the cyclic yield strain.

Concept of “Cyclic Yield Strain” or “Cyclic Reference Strain”

To measure the liquefaction resistance of sandy soil, the cyclic triaxial experiments (isotropically consolidated) are conducted 2-4 times by various cyclic stress ratio, $R_L = \sigma_d / (2\sigma'_0)$, where σ_d and σ'_0 denote a single amplitude of axial stress, and initial confining stress, respectively. For instance, a particular cyclic stress ratios, e.g. $R_L = 0.20$, applied to the sample, as illustrated in Figure 1(a), in order to produce different values of single amplitude of axial strain, ϵ_a , i.e. 0.75%(a'), 1.25%(b'), 2.5%(c'), 5%(d'). After similar experiments are repeated with several cyclic stress ratios, a set of curved lines is obtained by connecting the points of the same axial strain amplitude as shown in Figure 1(a).

It should be noted that 100% pore pressure build-up occurs almost concurrently with 2.5% single amplitude of axial strain, and 10 or 20 cycles of uniform loading can be representative of the strong earthquake with a magnitude of 7½. Thus, it has been common practice to perceive the cyclic stress ratio, which is the value of the cyclic strength determined by the curved line indicative of 2.5% single-amplitude axial strain at 20th cycle, as the liquefaction triggering. To intersect a line perpendicular to number-of-cycle axis at twentieth cycle and four curved lines, the points, i.e. a, b, c and d, are made as a function of particular cyclic stress ratio, e.g. $R_L = 0.15$, as shown in Figure 1(a). Then, it is feasible to set up by connecting those points in the plot of cyclic stress ratio versus axial strain, as shown in Figure 1(b) which can generally be consider as a kind of non-linear stress-strain model.

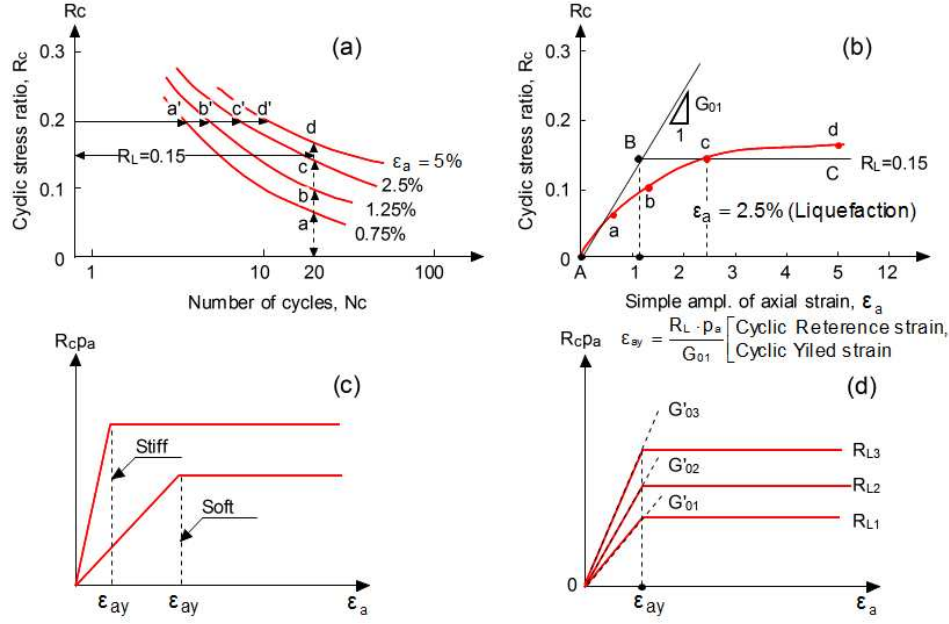


Figure 1. Schematic diagrams of the “reference strain” or “yield strain” in cyclic loading.

Based on the elasto-plastic theory, bi-linear lines can approximately be representative of the non-linear stress-strain relation. As shown in Figure 1(b), elastic behavior is related to the line passing through zero point with slop, G_0 , and plastic behavior is associated with the line being the level of particular cyclic stress ratio, e.g. $R_L=0.15$. The corresponding axial strain of point B, which results from intersection of two asymptotic lines, may be considered as a kind of “reference strain” or “yield strain” in cyclic loading. Based on Figure 1(b), cyclic yield strain or cyclic reference strain, ϵ_{ay} , can be defined by Equation 1, hereafter the expression of cyclic yield strain is utilized as ϵ_{ay} in this paper. In order to make this parameter a non-dimensional value, atmospheric pressure, $P_a=98 \text{ kN/m}^2$, is multiplied by the cyclic stress ratio.

$$\epsilon_{ay} = \frac{R_L \cdot p_a}{G_{01}} \quad (1)$$

Where, G_{01} denotes the value of G_0 at the atmospheric pressure. The physical interpretation of cyclic yield strain is shown in Figure 1(c); if the value of ϵ_{ay} is small, then the soil is considered as a material with “soft” behavior which may be indicative of an old aged deposit, whereas the soil possesses “stiff” behavior which can be representative of a new aged deposit if the value of ϵ_{ay} is high. The level of softness or stiffness for a given soil could be the same if the value of ϵ_{ay} remains constant as shown in Figure 1(d).

Correlation of Cyclic Yield Strain and Shear Wave Velocity

Based on the dynamic property of soil, the initial shear modulus, G_0 , can be derived from shear wave velocity, V_s , by this Equation ($G_0 = \frac{\rho}{g} V_s^2$), where g is 9.8 m/sec^2 , and ρ is bulk unit weight. Since shear modulus at atmospheric pressure, G_{01} , is utilized in Equation 2, shear wave velocity should be normalized to V_{s1} by being multiplied by $(P_a/\sigma'_v)^{0.25}$, where σ'_v denotes effective overburden pressure at a particular depth, and P_a is equal to 98 kN/m^2 .

$$G_{01} = \frac{\rho}{g} V_{s1}^2 \quad (2)$$

By substituting Equation 2 into Equation 1 yields Equation 3 which can practically be utilized in the evaluation of cyclic yield strain.

$$\varepsilon_{ay} = \frac{R_L \cdot p_a}{G_{01}} = \frac{R_L \cdot p_a}{\rho/g \cdot V_{s1}^2} \quad (3)$$

Undisturbed Specimens for Measuring Cyclic Strain

To determine the value of ε_{ay} , an extensive experimental program was carried out in the field as well as in the laboratory on undisturbed and disturbed specimens. For this aim, the areas of Asahi city in Chiba prefecture, which is along the costal line of Pacific Ocean, and Ohya tailings dam site, which were affected by the 2011 East Japan earthquake, have been considered as earthquake-induced liquefaction zones in this study.

Soil borings were carried out at six selected locations of this area. 6 detailed soil profiles were obtained on basis of geotechnical investigation. In order to extract undisturbed specimens, three different samplers, i.e. the thin-wall tube sampler, the triple tube sampler and the Denison sampler, were utilized based on the depth and the type of soil.

Procedure of Cyclic Triaxial Test and V_S Measurement Laboratory

Tube samples from Asahi site contained about 30% fines and thus were hung vertically overnight at the site to drain excess water. The partially saturated sands in the tubes were frozen in the field.

After setting up the frozen specimens enclosed in rubber membrane, 100 mm long and 50 mm in diameter, in the chamber of cyclic triaxial, it was permitted to thaw approximately 1-2 hours while employing a low vacuum of 20 kN/m². Carbon dioxide was gradually percolated into the specimens for 30-60 minutes depending on the amount of fines content. Next, the de-aired water was permitted to enter the specimens so that the B-value became more than 96% by applying 200 kN/m² back pressure. Then, the specimens were isotropically consolidated at specified effective confining pressure based on the depth of undisturbed specimens in soil profile. The consolidation of specimens was fully accomplished in a drained condition for approximately 30-90 minutes, whereupon the V_S was measured twice by means of a new device -termed "shear wave monitoring apparatus"- which is attached to the cyclic triaxial apparatus, and is somewhat like bender element in practice. In contrast to bender element, it makes infinitesimally torsional movement to send an impulse through the sample without any disturbance by entering small tools into the sample as has been implemented in bender element test.

The specimens were subjected to cyclic axial loading in the form of 1 Hz sinusoidal wave in undrained condition until the axial deformation reached to 10%. Once the cyclic loading was finalized, the water inside the specimen was permitted to drain out in order to measure its volume change after approximately 30-60 minutes drainage.

Outcomes of Experiments on Undisturbed Specimens

The outcomes of cyclic loading experiment on the undisturbed specimens from Asahi site and the undisturbed specimens from Ohya tailings dam site failed in 2011 earthquake (Ishihara et al. 2015) are depicted in Tables 1 and 2. Some of experiments were carried out by Chiba Eng. Co. without V_S measurement in the laboratory as shown in Table 1. Consequently, V_S values of in-situ measurement are utilized, whereas the value of V_{S1} related to laboratory measurements was calculated by the value of G_{01} measured by laboratory tests. However, some other experiments were performed by Kiso-Jiban consultants Co. with cyclic triaxial apparatus equipped by shear wave monitoring apparatus which measures shear wave velocity in laboratory as shown in Table 2, whereas the values of V_{S1} related to laboratory and field measurements was calculated by the values of V_S measured by Laboratory and field tests. In these tables, specimens related to fills and once-liquefied alluviums are separated from those associated with non-liquefied alluvial and diluvial deposits. Moreover, in the columns of V_S and V_{S1} , laboratory measurements of V_S are distinguished from field measurements by denoting “L” and “F” as laboratory and field, respectively. In tables 1 and 2, the once-liquefied deposits or fills are denoted by “ ℓ ” and non-liquefied old deposits are denoted by “n”.

Table 1. Undisturbed specimens from Asahi with V_S measurement in the field

| Site | Sample number | Age | Depth (m) | σ'_v (kpa) | N-value | N1-value | FC (%) | V_S (m/sec) | V_{S1} (m/sec) | G_{01} (Mpa) | R_L | $\epsilon_{ay} = \frac{R_L \cdot Pa}{G_{01}}$ |
|--------|---------------|-----------------|-----------|-------------------|---------|----------|--------|---------------|------------------|-----------------|-------|---|
| HB-S-1 | HB-S-1 (S-1) | Fill ℓ | 1.0-3.8 | 30 | 7 | 9 | 0.9 | F160 | L168 F216 | L52.2 F86.3 | 0.304 | L** 5.82×10^{-4} F* 4.48×10^{-4} |
| | HB-S-1 (S-4) | As ⁿ | 7.0-10.9 | 87 | 25 | 27 | 1 | F240 | L189 F248 | L65.7 F116.0 | 0.282 | L 4.29×10^{-4} F 2.43×10^{-4} |
| | HB-S-1 (S-7) | As ⁿ | 15.0-16.9 | 150 | 21 | 26 | 10.7 | F190 | L201 F172 | L76.4 F55.8 | 0.276 | L 3.61×10^{-4} F 4.95×10^{-4} |
| | HB-S-1 (S-9) | As ⁿ | 22.0-23.7 | 215 | 12 | 8 | 9.6 | F190 | L208 F157 | L81.8 F46.5 | 0.276 | L 3.37×10^{-4} F 5.94×10^{-4} |
| JG-S-1 | JG-S-1 (S-1) | As ⁿ | 5.0-8.0 | 74 | 25 | 29 | 2.2 | F180 | L150 F194 | L42.9 F71.1 | 0.176 | L 4.10×10^{-4} F 2.48×10^{-4} |
| | JG-S-1 (S-4) | As ⁿ | 8.0-9.9 | 91 | 22 | 23 | 6.6 | F150 | L168 F154 | L53.1 F44.5 | 0.268 | L 5.05×10^{-4} F 6.02×10^{-4} |
| | JG-S-1 (S-6) | As ⁿ | 16.0-17.8 | 163 | 45 | 35 | 5.7 | F270 | L192 F239 | L69.6 F108.0 | 0.28 | L 4.02×10^{-4} F 2.59×10^{-4} |
| | JG-S-1 (S-8) | Ds ⁿ | 26.0-27.8 | 248 | 11 | 7 | 28.7 | F250 | L179 F199 | L73.4 F74.8 | 0.229 | L 3.12×10^{-4} F 3.06×10^{-4} |
| NH-S-1 | NH-S-1 (S-1) | Fill ℓ | 2.0-5.8 | 53 | 4 | 6 | 20.5 | F140 | L121 F164 | L27.3 F50.1 | 0.295 | L 10.8×10^{-4} F 5.89×10^{-4} |
| | NH-S-1 (S-4) | As ⁿ | 10.0-11.9 | 112 | 31 | 30 | 9.6 | F260 | L199 F253 | L75.3 F122.0 | 0.206 | L 2.73×10^{-4} F 1.69×10^{-4} |
| | NH-S-1 (S-6) | Ds ⁿ | 26.0-27.0 | 244 | 4 | 3 | 84 | F150 | L165 F120 | L51.4 F27.2 | 0.246 | L 4.78×10^{-4} F 9.04×10^{-4} |

L: Laboratory, F: Field, ℓ : Liquefied Alluvium or Fills,
n: non-liquefied, As: Alluvial sand, Ds: Diluvial sand

Table 2. Undisturbed specimens from Asahi with V_{S1} measurement in the laboratory & field

| Site | Sample number | Age | Depth (m) | σ'_{v0} (kpa) | N-value | N_1 -value | FC (%) | V_{S1} (m/sec.) | V_{S1} (m/sec.) | G_{01} (Mpa) | R_L | $\epsilon_{ay} = \frac{R_L \cdot p_a}{G_{01}}$ |
|--------|---------------|-------------------|-----------|----------------------|---------|--------------|--------|-------------------|-------------------|------------------|-------|--|
| HG-S-1 | HG-S-1 (S-1) | As ^l | 2.0-3.0 | 25 | 4 | 6 | 11.8 | L 127 F 110 | L 180 F 156 | L 59.5 F 47.6 | 0.23 | L 3.86×10^{-4} F 4.83×10^{-4} |
| | HG-S-1 (S-4) | As ^l | 4.0-5.0 | 60 | 6 | 8 | 12.1 | L 115 F 115 | L 131 F 131 | L 31.5 F 31.5 | 0.3 | L 9.52×10^{-4} F 9.52×10^{-4} |
| | HG-S-1 (S-1) | As ⁿ | 4.0-6.0 | 60 | 6 | 8 | 25.4 | F 110 | F 125 | F 28.7 | 0.299 | F 10.4×10^{-4} |
| | HG-S-1 (S-5) | As ⁿ | 7.0-10.0 | 87 | 18 | 19 | 26.2 | F 170 | F 176 | F 45.4 | 0.281 | F 4.80×10^{-4} |
| | HG-S-1 (S-11) | Ds ⁿ | 18.0-20.0 | 180 | 10 | 7 | 52.4 | F 180 | F 155 | L 26.7 F 45.4 | 0.284 | F 6.25×10^{-4} |
| | HG-S-1 (S-11) | Ds ⁿ | 18.0-20.0 | 180 | 10 | 7 | 42.3 | L 138 F 180 | L 119 F 155 | L 61.9 F 45.4 | 0.28 | L 10.5×10^{-4} F 6.17×10^{-4} |
| SN-S-1 | SN-S-1 (S-6) | Fill ^l | 1.0-2.0 | 20 | 5 | 11 | 1.9 | L 121 F 100 | L 181 F 149 | L 61.9 F 41.7 | 0.35 | L 5.65×10^{-4} F 8.39×10^{-4} |
| | SN-S-1 (S-10) | Ds ⁿ | 24.0-26.1 | 215 | 23 | 16 | 9 | L 211 F 220 | L 174 F 182 | L 57.8 F 66.3 | 0.24 | L 4.15×10^{-4} F 3.62×10^{-4} |
| SN-S-2 | SN-S-2 (S-6) | As ⁿ | 13.0-14.0 | 115 | 26 | 24 | 5 | L 209 F 220 | L 202 F 182 | L 76.3 F 84.8 | 0.23 | L 3.01×10^{-4} F 2.71×10^{-4} |
| | SN-S-2 (S-7) | As ⁿ | 20.1-20.8 | 190 | 79 | 57 | 1.3 | L 218 F 250 | L 186 F 213 | L 65.3 F 86.4 | 0.22 | L 3.37×10^{-4} F 2.55×10^{-4} |
| | SN-S-2 (S-9) | As ⁿ | 20.8-21.8 | 198 | 79 | 57 | 5 | L 134 F 250 | L 113 F 211 | L 24.1 F 84.0 | 0.2 | L 8.30×10^{-4} F 2.38×10^{-4} |

l: Liquefied, n: non-liquefied, L: Laboratory, F: Field
As: Alluvial sand, Ds: Diluvial sand

Correlation Between Cyclic Strength and Shear Wave Velocity

Since new fills or liquefied sands are totally different from old aged sands in terms of cementation, stiffness and strength, their correlations of cyclic strength and V_{S1} may be separated into two groups. Therefore, the values of V_{S1} , measured in field and laboratory, versus liquefaction resistance were plotted based on Tables 1 and 2 as shown in Figures 2 and 3. Regarding the values of V_{S1} , there appears no clearly discernible tendency of differentiating between the data from the field and those from the laboratory tests. Thus, the data from these two sources are joined by a horizontal line connecting the two points in the diagram.

Two distinctive curves may be proposed on basis of their age by means of the experimental data of Ohya dam site identified by the solid and open reverse triangle symbols, and of Asahi city site identified by the solid and open rectangle symbols in Figures 4 and 5, respectively. The characteristics of these curves are explained below:

- (1) The chart of cyclic strength versus V_{S1} for new age deposits based on the undisturbed specimens from the new fills or liquefied sands is presented in Figure 5. The curved line drawn through the average points is represented by $R_L = 0.9 \times 10^{-5} V_{S1}^2$ and the corresponding cyclic yield strain is 4.6×10^{-6} . Since there were relatively few data to indicate the regression line reliably as shown in Figure 2, a series of experiments was conducted on the reconstituted specimens from undisturbed specimens tested previously in this project and Nagoya sand with various fines contents, i.e. 0%, 10% and 30%. The results of those specimens as shown in the Figure 4 are accurately consistent with the proposed line.

- (2) The chart of cyclic strength versus V_{S1} for old age deposits is presented in Figure 3. The curved line passing through average points of data is represented by $R_L = 0.68 \times 10^{-5} V_{S1}^2$, and the corresponding cyclic yield strain is 3.6×10^{-4} . With regard to this point, the values of V_{S1} measured in field and laboratory were given equal weighting. Thus, the proposed line is passed through the average points of in situ and laboratory V_{S1} .

Correlation of V_S -Based Liquefaction Chart for New and Old Aged Deposits

The average curve pertaining to new man-made deposits or reconstituted samples which is quoted from Figure 2, along with the average curve in Figure 3 representative of the correlation for old aged deposits. It can be seen that the relation for aged deposits is represented by the curve with a parameter of $\epsilon_{ay} = 3.6 \times 10^{-4}$ which is smaller than the corresponding value of $\epsilon_{ay} = 4.6 \times 10^{-4}$ for new or artificial deposits. This implies that aged deposits possessed stiff characteristics, as compared to soft nature of newly placed or artificial deposits.

There are several charts proposed for the relationship between the cyclic strength and shear wave velocity V_{S1} . These are summarized by Andrus and Stokoe (2000) as reproduced in the diagram of Figure 5 in which the two lines proposed in the present study are superimposed. It appears that the majority of the data sets complied hitherto are those from field observations and measurements. In this view, the proposed curve pertaining to old deposits with $\epsilon_{ay} = 3.6 \times 10^{-4}$ seems to show a reasonable level of coincidence particularly with the relations proposed by Tokimatsu and Uchida (1990) and Robertson et al. (1992).

Conclusions

An attempt was made to develop a particular relationship between the cyclic strength of sandy soils and the shear wave velocity in terms of new and old aged deposits. As one of the factors, the effect of aging was investigated in this paper on the basis of the cyclic triaxial test results. The tests were performed on undisturbed specimens recovered from liquefied deposits as well as non-liquefied deposits during the 2011 East Japan Earthquake. The tests consisted of non-destructive measurements of shear wave velocity, followed by the cyclic loading to cause liquefaction. By taking the ratio between the cyclic resistance causing liquefaction in 20 cycles and the square of the shear wave velocity, what might be called “cyclic yield strain” or “cyclic reference strain” was defined. It was shown that the higher the cyclic yield strain, the softer the soil is and the lower values indicate the stiffer nature of soils.

As a result of the multiple series of the tests, undisturbed specimens from old aged alluvial deposits were found to exhibit the cyclic yield strain which is lower than those from once-liquefied or artificially reclaimed soil deposits. Similar results of tests were obtained for reconstituted samples. It may be suggested that different relations be used to establish the correlation between the cyclic resistance of in-situ soils and the shear wave velocity with respect to new and old deposits. Thus, the relationship between these two quantities as determined via the relevant cyclic yield strain may be considered to be useful for assessing the liquefaction resistance of in-situ deposits through measurements of the shear wave velocity.

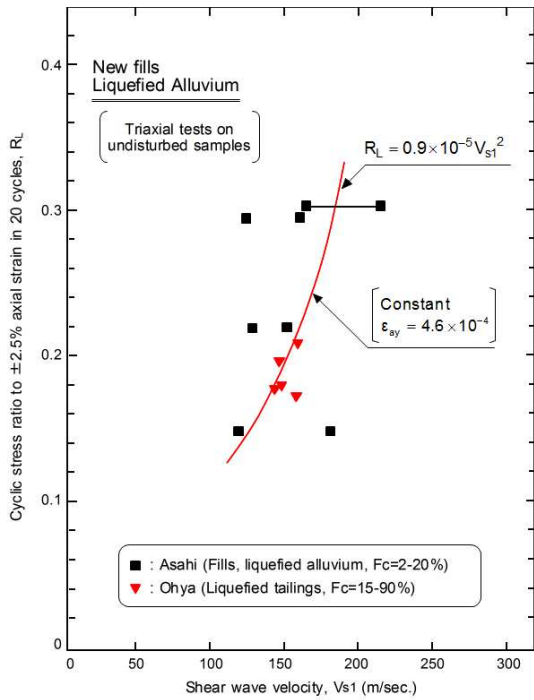


Figure 2. Correlation between the cyclic strength and shear wave velocity for intact specimens from new aged deposits.

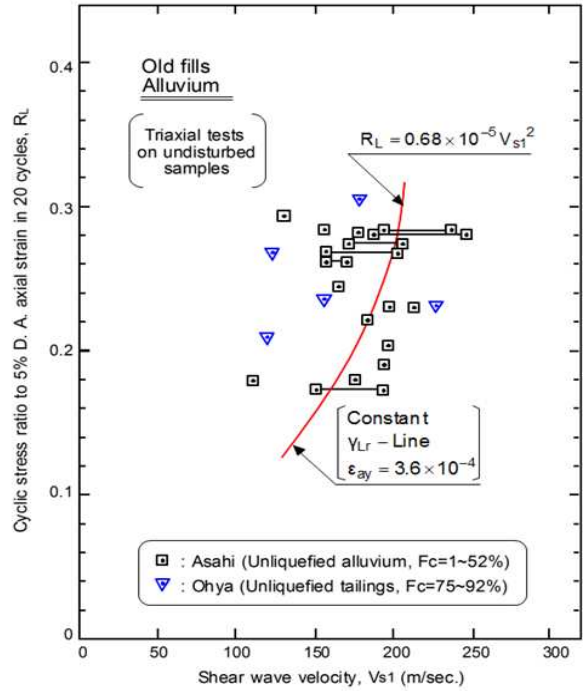


Figure 3. Correlation between the cyclic strength and shear wave velocity for intact specimens from old aged deposits.

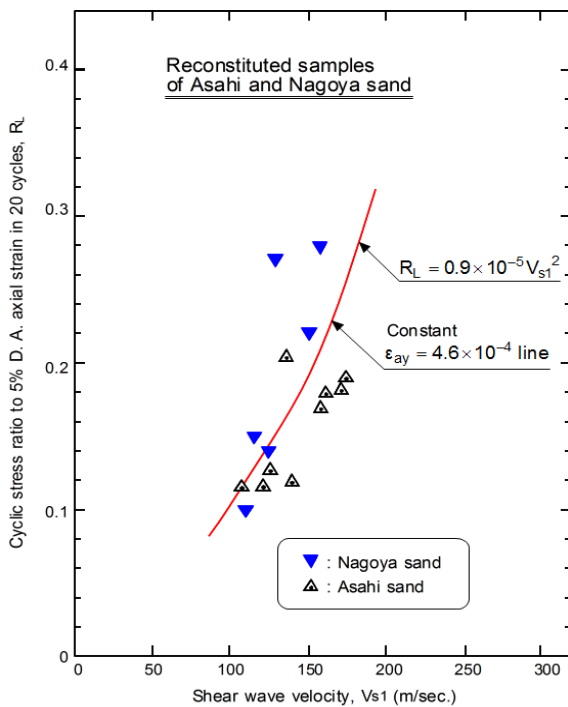


Figure 4. Correlation between cyclic strength and shear-wave velocity for reconstituted specimens

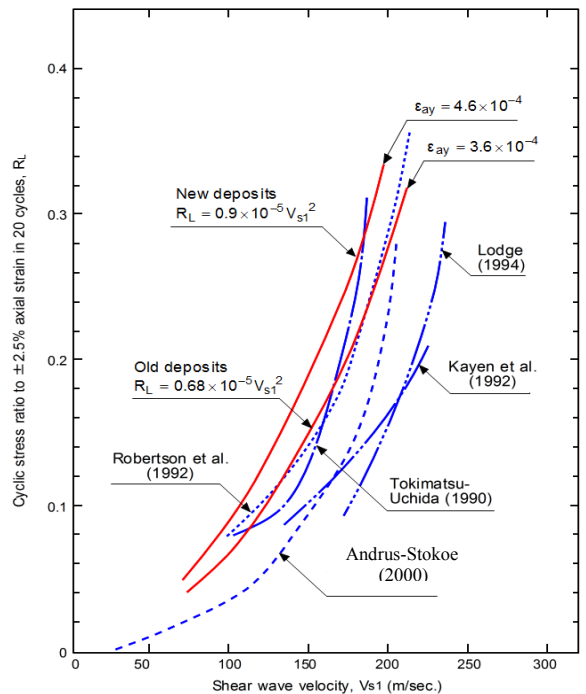


Figure 5. Summary V_s -based liquefaction charts for new or old aged sand deposits (Reproduced from the figure by Andrus and Stokoe, 2000)

References

Andrus RD and Stokoe KHIII. Liquefaction Resistance of Soils from Shear-Wave Velocity. *Journal of Geotechnical and Geoenvironmental Engineering*, ASCE; 2000; **126**(11): 1015-1025.

Dobry R, Powell DJ, Yokel FY, and Ladd, RS. Liquefaction Potential of Saturated Sand – The Stiffness Method. *Prof. 7th World Conference on Earthquake Engineering*, Istanbul, Turkey; 1980, Vol. 3, pp. 25-32.

Ishihara K, Ueno K, Yamada S, Yasuda S, and Yoneoka T. Breach of Tailings Dam in the 2011 Earthquake in Japan. *International Journal of Soil Dynamics and Earthquake Engineering*; 2015, Vol. **68**, pp. 3-22.

Robertson PK, Woeller DJ and Finn WDL. Seismic Cone Penetration Test for Evaluating Liquefaction Potential under Cyclic Loading. *Canadian Geotechnical Journal*; 1992, Vol. **29**, pp. 686-695.

Tokimatsu K, and Uchida A. Correlation between Liquefaction Resistance and Shear Wave Velocity. Soils and Foundations, *Journal of Japanese Geotechnical Society*; 1990, Vol. **30**, No. 2, pp. 33-42.